Coordinated Polar Localization of Auxin Efflux Carrier PIN1 by GNOM ARF GEF

Thomas Steinmann,[1] Niko Geldner,[1] Markus Grebe,[1] Stefan Mangold,[1] Catherine L. Jackson,[2] Sonia Paris,[3] Leo Gälweiler,[4] Klaus Palme,[4] Gerd Jürgens[1]*

The plant hormone auxin is transported in a polar manner along the shoot-root axis, which requires efflux carriers such as PIN1. Asymmetric localization of PIN1 develops from a random distribution in *Arabidopsis* early embryogenesis. Coordinated polar localization of PIN1 is defective in *gnom* embryos. GNOM is a membrane-associated guanine-nucleotide exchange factor on ADP-ribosylation factor G protein (ARF GEF). Thus, GNOM-dependent vesicle trafficking may establish cell polarity, resulting in polar auxin transport.

Polar auxin transport has been implicated in a variety of developmental processes, including phototropism, gravitropism, apical dominance, root formation, and vascular tissue patterning (*1*, *2*). These vectorial processes require coordinated polar organization of cells that is reflected in the localization of putative auxin efflux carrier, PIN1, at the basal boundary of vascular cells in the axis of *Arabidopsis* plants (*3*). How this coordinated cell polarity originates during development is not known but may be presumed to arise during apical-basal axis formation in embryogenesis. Mutations in two *Arabidopsis* genes, *MONOPTEROS* (*MP*) and *GNOM* (*GN*), cause specific axial defects. The *MP* gene encodes a transcription factor binding to auxin-response elements that is involved in cell axialization and polar auxin transport (*4*, *5*). The earliest defect observed in *mp* embryos was an abnormal division of the apical daughter cell of the zygote that gives rise to almost the entire embryo (*6*). *gn* embryos deviate from wild type already at the zygote stage, show variable expression of apical marker gene *LTP*, and give rise to seedlings that lack or have a variably compromised apical-basal axis (*7*, *8*). Bisected *gn* seedlings are unable to form polar root organization but produce disorganized callus growth (*7*). Here we analyze the role of GNOM, an ARF GEF, in the establishment of coordinated polar localization of PIN1 in embryogenesis.

In the course of wild-type embryogenesis, PIN1 expression underwent dynamic changes, accompanied by an increasingly polar localization in groups of adjacent cells (Fig. 1). At the 16-cell stage, all cells of the embryo proper accumulated PIN1 at their inner cell boundaries (Fig. 1A). PIN1 first showed polar localization at mid-globular stage: The four innermost cells in the lower part of the embryo accumulated PIN1 at their basal boundary toward the future root tip (Fig. 1B, asterisk). PIN1 expression was gradually narrowed down to vascular precursor cells, both in the developing cotyledons and in the embryo axis (Fig. 1, C and I). From the heart stage, the vascular precursor cells accumulated PIN1 at their basal boundary facing the root pole (Fig. 1C, inset). The opposite polarity was observed in the epidermal cell layer of cotyledonary primordia (Fig. 1D, inset).

To determine how the coordinated polar localization of PIN1 is established, we analyzed *mp* and *gn* embryos, which are defective in apical-basal patterning (*4*, *7*). Despite early defects in the basal half (*4*), *mp* embryos displayed coordinated polar localization of PIN1 similar to that of wild type, in both the basal orientation of inner cells (Fig. 1, K and L) and the opposite orientation in the epidermis (Fig. 1M), suggesting that the auxin-response transcription factor MP is not required. In *gnom* embryos, PIN1 expression developed in a different manner, eventually resulting in strong labeling of clusters of presumptive vascular precursor cells (Fig. 1, E to G, J). PIN1 localization appeared disorganized, with no coordinated polar localization in inner cells (Fig. 1, F and G). Individual cells within the *gnom* embryo displaying polar PIN1 distribution were not aligned with one another, nor with the axis of the embryo (Fig. 1G, inset). Only the epidermis displayed a more organized PIN1 localization (Fig. 1 H, inset). These results suggest that GNOM function is required for establishment of coordinated cell polarity in embryo axis formation.

GNOM shows extensive sequence simi-

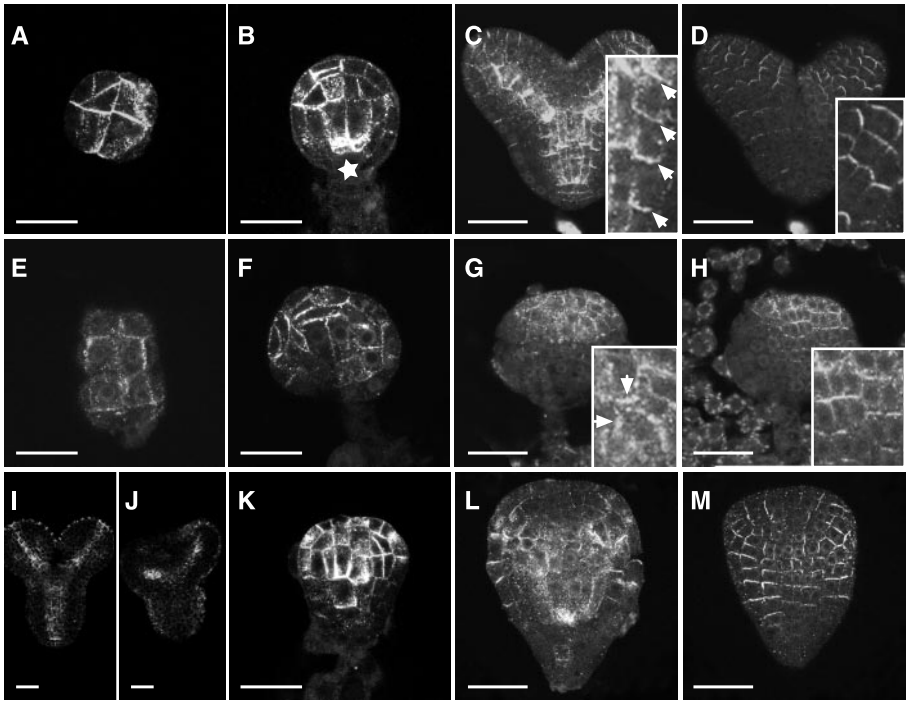

Fig. 1. PIN1 localization in early embryogenesis. (**A** to **D**, **I**) Wild-type, (**E** to **H**, **J**) *gnom*, and (**K** to **M**) *monopteros*. Stages of embryogenesis (*25*): (A and E) early-globular, (B, F, K) mid-globular, (C, D, G, H, L, M) mid-heart, and (I and J) early/mid-torpedo. Asterisk (B) and arrows (insets in C and G) mark polar localization of PIN1. (A to C, E to G, I to L) Internal optical sections; (D, H, M) surface views; apical end of embryo is up. Bars, 20 μm. Images were obtained by confocal microscopy (*26*).

[1]Entwicklungsgenetik, Zentrum für Molekularbiologie der Pflanzen, Universität Tübingen, Auf der Morgenstelle 1, D-72076 Tübingen, Germany. [2]Service de Biochimie et Génétique Moléculaire, Commissariat à l'Energie Atemique/Saclay, F-91191 Gif-sur-Yvette, France. [3]Institut de Pharmacologie Moléculaire et Cellulaire du Centre National de la Recherche Scientifique, Sophia Antipolis, F-06560 Valbonne, France. [4]Max-Delbrück-Laboratorium in der Max-Planck-Gesellschaft, D-50829 Köln, Germany.

*To whom correspondence should be addressed. E-mail: gerd.juergens@uni-tuebingen.de

larity to two functionally redundant ARF GEFs from budding yeast, Gea1p and Gea2p (*9*, *10*). Expression of full-length GNOM protein (*11*) rescued *gea1-19 gea2*Δ temperature-sensitive yeast cells (Fig. 2A). Thus, GNOM has functional similarity to these two yeast ARF GEFs. We determined ARF GEF activity of GNOM by an in vitro guanosine diphosphate/guanosine triphosphate (GDP/GTP) exchange assay (*10*, *12*) (Fig. 2B). GNOM protein partially purified from yeast stimulated GTP binding to recombinant mammalian ARF1 about threefold as compared with a control fraction from vector-transformed yeast (*13*). This stimulation of GDP/GTP exchange was in the range reported for other large ARF GEFs (*10*) and, furthermore, was inhibited by the fungal toxin brefeldin A (BFA), a specific inhibitor of large ARF GEFs (*10*), in a concentration-dependent manner (Fig. 2C). These results suggest that GNOM is a BFA-sensitive ARF GEF.

To gain insight into its in vivo function, we analyzed the location of GNOM protein in plant tissue. Antiserum raised against the Sec7 domain of GNOM (*14*, *15*) detected a 165-kD band, which was absent from *gnom* alleles with splice site or early stop-codon mutations (Fig. 2D) (*7*, *9*, *16*). GNOM was expressed in different developmental stages, organs, and suspension cells (Fig. 2E). *gnom* suspension cells grew as well as wild-type cells, and trafficking of compartment-specific membrane markers was not altered in *gnom* embryos (*17*), suggesting that GNOM is not required for membrane trafficking in general cell growth.

The subcellular localization of GNOM protein was examined by differential ultracentrifugation (Fig. 2F). A fraction of GNOM was membrane-associated, although the *GNOM* coding sequence gave no indication of a membrane-interaction domain (*9*). GNOM was released by Triton X-100 but not by high salt concentrations or alkaline pH, suggesting a strong membrane association. In contrast to the KNOLLE syntaxin, an integral membrane protein (*15*), GNOM was solubi-

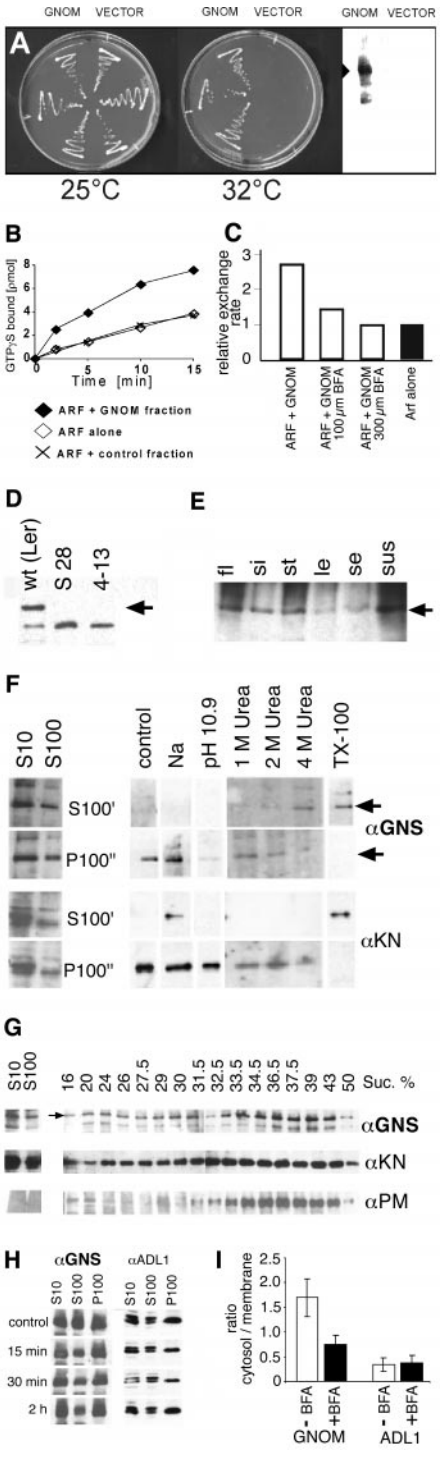

Fig. 2. Molecular characterization of GNOM protein. (**A**) Rescue of *gea1-19 gea2*Δ temperature-sensitive yeast by full-length GNOM protein [immunoblot (*15*), right]. Growth of independent transformants after 5 days. Vector: yeast transformed with empty vector (*11*). (**B** and **C**) In vitro GDP/GTP exchange assay (*12*). (B) Kinetics of GTPγS loading with or without GNOM fraction. Values were corrected for unspecific radioactivity binding of fractions without ARF. (C) Concentration-dependent BFA inhibition of exchange rate after 5 min. Assays contained equal amounts of ethanol as introduced by BFA addition. The experiment was repeated giving less than 10% deviation. (**D**) Protein immunoblot analysis of wild-type (Ler) and *gnom* seedling extract (*15*). Arrow marks 165-kD GNOM band. (**E**) Organ distribution of GNOM protein (arrow) in wild-type urea extracts. fl, flowers; si, siliques; st, stems; le, leaves; se, seedlings; sus, suspension cells. (**F** and **G**) Cell fractionation (*15*). (F) Membrane association of GNOM protein. Samples of supernatant (S10) were centrifuged at 100,000*g* for 1 hour to give soluble fractions (S100) and pellets. Pellets were resuspended in original volumes of homogenization buffer without additives (control); with 1 M NaCl (Na); 0.1 M Na_2CO (pH 10.9); 1, 2, or 4 M urea; or 1% Triton X-100 (TX-100), and after 30 min centrifuged again at 100,000*g* for 90 min, giving wash fractions S100′ and pellets. This procedure was repeated to give washed pellets P100″. (G) Sucrose density centrifugation. Pellets (P100) were resuspended in homogenization buffer and centrifuged through a linear 15 to 45% sucrose gradient at 107,000*g* at 4°C for 18 hours. Sucrose concentrations of fractions (top) were determined by refractometry before protein immunoblot analysis (*15*). (**H** and **I**) BFA treatment of suspension cells. (H) Time course. BFA (50 μM) in DMSO; controls, DMSO only. Cell fractionation after incubation times is indicated. Antibody concentrations: anti-GNS (αGNS), 1:4000 and as in (*15*). (I) Quantitation of BFA effect (*20*). Cells were treated with 100 μM BFA for 30 min. Other conditions were as in (H).

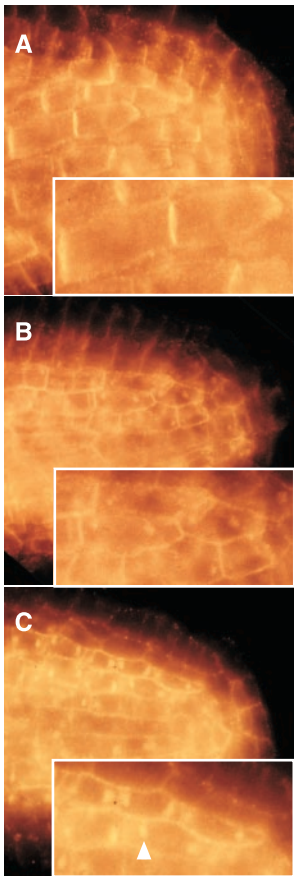

Fig. 3. PIN1 localization in BFA-treated developing lateral roots of wild-type seedlings. (**A**) Control root showing polar localization of PIN1 (inset). (**B** and **C**) Loss of polar localization of PIN1 (inset, B) and formation of "BFA compartments" (arrowhead, inset, C) after (B) 30 min and (C) 2 hours of BFA treatment (*22*). Root tip is to the right.

lized with urea in a concentration-dependent manner (Fig. 2F). Thus, protein conformation appears to be essential for membrane association of GNOM. Immunolocalization of the GNOM protein gave no conclusive results (*16*). However, linear sucrose-density gradient centrifugation revealed GNOM protein in all fractions, suggesting association with multiple membrane compartments, as well as enrichment at the plasma membrane (Fig. 2G).

BFA and ARF GEF are thought to affect membrane trafficking in various organisms, including plants (*18*). We analyzed the subcellular distribution of GNOM protein in suspension cells treated with BFA (Fig. 2, H and I). The amount of cytosolic GNOM was rapidly reduced relative to the membrane-associated fraction, whereas partitioning of a control protein, the peripheral membrane protein ADL1 (*19*), was not changed over 2 hours. Quantitative analysis (*20*) indicated that the ratio of cytosolic to membrane-associated GNOM protein was reversed, in contrast to ADL1 (Fig. 2I). Thus, BFA had a specific effect on cytosolic GNOM, which suggests that GNOM is also an in vivo target of BFA action.

BFA treatment blocks auxin efflux activity (*21*), and lack of the BFA-sensitive GNOM ARF GEF interfered with coordinated polar localization of PIN1. We therefore analyzed the effect of BFA on PIN1 localization in developing lateral roots (*22*). PIN1 accumulated at cell boundaries facing the newly formed root tip (Fig. 3A). Short-term treatment with BFA disrupted PIN1 polar localization, resulting in PIN1 being equally distributed along the entire cell surface (Fig. 3B, inset; compare with 3A, inset). The PIN1 label gradually coalesced into patches inside the cell, which was much more pronounced after longer treatment, with label persisting around the cell surface (Fig. 3C, inset). This result suggests that the steady-state polar localization of PIN1 involves continuous activity of BFA-sensitive ARF GEF (or ARF GEFs).

Polar auxin flux requires coordinated polar organization of cell groups, which is reflected in the accumulation of the putative efflux carrier PIN1 at downstream cell boundaries (*3*). Our results indicate that this polar localization is a steady state that requires BFA-sensitive membrane trafficking for maintenance. Polar localization of PIN1 along the apical-basal axis is gradually established from a nonoriented distribution in the very young embryo, suggesting a positive-feedback loop along the lines of the canalization hypothesis of Sachs (*2*). We suggest that the BFA-sensitive GNOM ARF GEF regulates vesicle trafficking required for the coordinated polar localization of auxin efflux carriers which in turn determines the direction of auxin flow. Failure to establish polar auxin transport would thus cause the axis defects observed in *gnom* embryos. Indeed, blocking auxin flow in *Brassica juncea* globular embryos results in phenocopy of *gnom* seedlings (*23*).

References and Notes

1. F. W. Went, *Rec. Trav. Bot. Neerl.* **25**, 1 (1929).
2. T. Sachs, *Development* (suppl. 1), 83 (1991).
3. L. Gälweiler *et al.*, *Science* **282**, 2226 (1998).
4. T. Berleth and G. Jürgens, *Development* **118**, 575 (1993).
5. G. K. Przemeck, J. Mattsson, C. S. Hardtke, Z. R. Sung, T. Berleth, *Planta* **200**, 229 (1996); T. Ulmasov, G. Hagen, T. J. Guilfoyle, *Science* **276**, 1865 (1997); C. S. Hardtke and T. Berleth, *EMBO J.* **17**, 1405 (1998).
6. T. Hamann, U. Mayer, G. Jürgens, *Development* **126**, 1387 (1999).
7. U. Mayer, G. Büttner and G. Jürgens, *ibid.* **117**, 149 (1993).
8. C. W. Vroemen *et al.*, *Plant Cell* **8**, 783 (1996).
9. M. Busch, U. Mayer, G. Jürgens, *Mol. Gen. Genet.* **250**, 681 (1996).
10. A. Peyroche, S. Paris, C. L. Jackson, *Nature* **384**, 479 (1996).
11. Yeast strain CJY052-10-2/pgea1-19 (*10*) (permissive temperature 25°C, restrictive temperature 30°C) was transformed with pYX242 alone, and the rescue plasmid containing the entire open reading frame of *GNOM* amplified from plasmid c96 (*9*) and directionally ligated into yeast expression vector pYX242 (Invitrogen) by using 5' Nco I and 3' Mlu I sites.
12. M. Franco, P. Chardin, M. Chabre, S. Paris, *J. Biol. Chem.* **270**, 1337 (1995).
13. An NH_2-terminally His-tagged version of pYX242-*GNOM* was constructed by three-point ligation, in which a 5′ Eco RI, 3′ Nco I 6xHis adapter were inserted together with a 5′ Nco I, 3′ Mlu I–digested full-length GNOM fragment into an Eco RI, Mlu I–digested vector. Transformants of yeast strain EGY48 with pYX242-*His-GNOM* were grown at 30°C on −Leu yeast selective medium and proteins were purified as described (*10*). Cells were resuspended in 50 ml of buffer A plus proteinase inhibitors and lysed by grinding in liquid nitrogen in the presence of glass beads. Expressed proteins were purified by Ni–nitrilotriacetic acid affinity chromatography, and the control fraction from vector-transformed yeast strain contained the same contaminating bands as the GNOM fraction [assessed by silver staining (*24*)].
14. Nucleotides 3163 to 3631 of the *GNOM* cDNA c96 (*9*) were expressed as NH_2-terminal 6xHis-tag fusion protein in *Escherichia coli* (Qiaexpress, Qiagen) and purified for immunization of rabbits (*15*).
15. M. H. Lauber *et al.*, *J. Cell. Biol.* **139**, 1485 (1997).
16. The antiserum cross-reacted with other proteins. The same response was observed for an antiserum against the COOH-terminal region of GNOM (*24*). Attempts to purify the antisera by affinity chromatography and immunoadsorption did not remove the cross-reacting antibodies, and no distinct differences in immunolocalization of GNOM were observed between wild-type and *gnom* mutant cells (*24*).
17. The cell plate–specific KNOLLE syntaxin and the plasma membrane H^+-ATPase (adenosine triphosphatase) (*15*) were found by immunolocalization to accumulate at their respective membrane compartments in wild-type and *gnom* embryos (*24*).
18. A. Peyroche *et al.*, *Mol. Cell* **3**, 275 (1999); J. Lippincott-Schwartz, L. C. Yuan, J. S. Bonifacino, R. D. Klausner, *Cell* **56**, 801 (1989); B. Satiat Jeunemaitre and C. Hawes, *J. Cell Sci.* **103**, 1153 (1992).
19. J. M. Park *et al.*, *Plant Physiol.* **115**, 763 (1997).
20. Signals on protein immunoblots from four experiments were scanned with a Storm Phosphoimager (Molecular Dynamics) and quantitated with Imagequant.
21. A. Delbarre, P. Mueller, J. Guern, *Plant. Physiol.* **116**, 833 (1998); D. A. Morris and J. S. Robinson, *Planta* **205**, 606 (1998).
22. Seven-day-old seedlings were incubated in liquid growth medium containing 100 μM BFA or an equal volume of dimethyl sulfoxide for 30 min or 2 hours, fixed for 30 min, and processed on gelatin-coated slides as described (*15*). Antibody incubation was for 4.5 hours with vacuum infiltration for 10 min at the beginning of each step. Photographs were taken with a Zeiss microscope (Axiophot).
23. K. Hadfi, V. Speth, G. Neuhaus, *Development* **125**, 879 (1998).
24. T. Steinmann *et al.*, data not shown.
25. G. Jürgens and U. Mayer, in *EMBRYOS. Colour Atlas of Development*, J. B. L. Bard, Ed. (Wolfe, London, 1994), pp. 7–21.
26. Immunofluorescence localization in whole-mount preparations was done as described (*15*). Primary antibody anti-PIN1 was diluted 1:150, and Cy3-conjugated anti-rabbit secondary antibody (Dianova) was diluted 1:600. Confocal laser-scanning microscopy was done with the TCS-NT program (Leica). Standard scanning conditions: 100× objective, 1- to 1.5-fold zoomed.

27. We thank M. Kientz for technical assistance, H. Schwarz for immunizing rabbits, W. Michalke for providing the anti-PM ATPase monoclonal antibody, A. Peyroche for constructing the *gea1-19* yeast strain, and T. Hamann, M. Heese, M. Hülskamp, T. Laux, and U. Mayer for critical reading. Funded by the Deutsche Forschungsgemeinschaft grant Ju179/3-4 and Leibniz Programm.

6 July 1999; accepted 2 September 1999